

PAPER

View Article Online
View Journal | View Issue



Cite this: *Environ. Sci.: Processes Impacts*, 2022, 24, 1790

Assessing residential indoor and outdoor bioaerosol characteristics using the ultraviolet light-induced fluorescence-based wideband integrated bioaerosol sensor

Yao S. Addor,^a Darrel Baumgardner,^b Dagen Hughes,^b Nicholas Newman,^{acd} Roman Jandarov^a and Tiina Reponen^{id} ^{*a}

We assessed and compared indoor and outdoor residential aerosol particles in a third-floor apartment from August through September 2020. The measurements were conducted using a direct-reading ultraviolet light-induced fluorescence (UV-LIF) wideband integrated bioaerosol spectrometer (WIBS). It measures individual particle light scattering and fluorescence from which particle properties can be derived. The number concentrations of total aerosol particles (TAP) and total fluorescent aerosol particles (TFAP) were significantly higher indoors. Daily and hourly TFAP mean concentrations followed the same trends as the TAP, both indoors and outdoors. The daily mean rank of the TFAP fraction (TFAP/TAP) was significantly higher indoors (23%) than outdoors (19%). Particles representing bacteria dominated indoors while particles representing fungi and pollen dominated outdoors. The mean volume-weighted median diameters for TFAP were 1.67 μm indoors and 2.09 μm outdoors. Higher TFAP fraction indoors was likely due to occupants' activities that generated or resuspended particles. This study contributes to understanding the characteristics of residential aerosol particles in situations when occupants spend most of their time indoors. Based on our findings, a large portion of all indoor aerosol particles could be biological (15–20%) and of respirable particle size ($\geq 95\%$). Using a novel direct reading UV-LIF-based sensor can help quickly assess aerosol exposures relevant to human health.

Received 25th April 2022
Accepted 29th August 2022

DOI: 10.1039/d2em00177b

rsc.li/espri

Environmental significance

Bioaerosols may have adverse impacts on the environment and human health. Built environments are of particular concern since people spend 90% of their time inside. However, real-time measurements of residential bioaerosols are lacking. In this study, we utilized a direct reading, light-induced fluorescent-based instrument to characterize bioaerosols indoors and outdoors of an occupied residential apartment. We found a relatively high proportion of fluorescent aerosol particles whose concentrations were higher indoors than outdoors. They were mostly $<2.5 \mu\text{m}$ in size. Fluorescent Type A particles (mostly bacteria) dominated indoors suggesting that human occupancy and activities were the main contributing factors. Given that residential indoor environments can have high concentrations of bioaerosols, real-time assessment can help detection and mitigation efforts.

Introduction

Bioaerosols are, by definition, airborne particles of biological origin. They are ubiquitous in the environment and are products of anthropogenic or natural sources. They can originate from plants (pollen, for example), animals, and microorganisms such as archaea, viruses, bacteria, fungi, or their metabolic

products and debris. Bioaerosol particles have a variety of shapes, from spherical to rod-fiber-like, and various sizes ranging from 10 nm to 100 μm .^{1–4} Exposure to bioaerosols is associated with adverse health effects spanning allergic reactions, infectious diseases, respiratory disorders, cardiovascular diseases, and cancer.^{1,2,5–17}

Traditional offline methods to quantify bioaerosols, such as cultivation and microscopic counting, are widely available and commonly used. These methods require prior sample collection and results are not immediately available. While relatively cost-effective and considered gold-standard methods, they are time-consuming, labor-intensive, and each method detects only a specific category of bioaerosol. Over the last few decades, ultraviolet light-induced fluorescence (UV-LIF) techniques have been developed to measure fluorescent aerosol particles (FAP)

^aUniversity of Cincinnati, Department of the Environmental and Public Health Sciences, Cincinnati, OH, USA. E-mail: Tiina.Reponen@uc.edu

^bDroplet Measurement Technologies LLC., 2400 Trade Centre Avenue, Longmont, CO 80503, USA

^cUniversity of Cincinnati, Department of Pediatrics, Cincinnati, OH, USA

^dCincinnati Children's Hospital Medical Center, Division of General and Community Pediatrics, Cincinnati, OH, USA

in real-time. These techniques take advantage of the fluorescence properties of bioparticles when excited at specific wavelengths of light. By providing a real-time and particle-by-particle resolution output, they allow the study of changes in aerosol properties at much higher temporal and spatial scales. Commonly targeted biofluorophores include metabolic mediators such as tryptophan, riboflavin, and nicotinamide adenine dinucleotide hydrogenase (NADH) and its phosphorylated derivative NADPH and are known to be widely conserved in microbial species and plants.^{18–24}

The built environment is a particular focus of our study given that people spend more than 90% of their time indoors.^{25–27} This situation has been obviously exacerbated by the COVID-19 pandemic restrictions, which could impact indoor air quality due to increased human presence and activities within this environment.^{21,28–31} Results from many outdoor studies have shown that COVID-19 shutdowns impacted the outdoor air quality by reducing the levels of pollutants such as PM_{2.5}, PM₁₀, CO, CO₂, NO_x, and SO₂.^{32–34} However, studies that evaluate and compare bioaerosols in residential indoor and outdoor environments during the COVID-19 pandemic are scarce. To date, the only study that evaluated bioaerosols indoors and outdoors simultaneously in a residential setting using the WIBS instrument is the one conducted by Li *et al.*³⁵ before the COVID-19 pandemic in 2019. They assessed the interrelations between indoor and outdoor bioaerosols in a bedroom under living conditions in Singapore and found that human occupancy was the main contributing factor in the increase of indoor bioaerosols. In 2017, Tian *et al.*³¹ measured TAP (total aerosol particles) and TFAP (total fluorescent aerosol particles) in a kitchen (indoors only) using a real-time Ultraviolet Aerodynamic Particle Sizer (UV-APS), and determined that occupant activities strongly influenced indoor TFAP levels. Nathu and collaborators³⁶ showed that human activities contribute to an increase in bioaerosol levels in indoor environments. They reported, for instance, that bedsheet changing was responsible for an increase in the bacterial concentration, that showering produced the highest increase in the concentration of fungi, fluorescent, and non-fluorescent particles, whereas walking increased pollen levels. Also, Nieto-Caballero and collaborators³⁷ assessed airborne fungi indoors and outdoors of occupied classrooms, before and after major public school renovations in Colorado, using an InstaScope (a fluorescent aerosol cytometer (FAC)) similar to the WIBS along with qPCR and *N*-acetylhexosaminidase (NAHA) detection. Due to the scarcity of data on the measurement of residential bioaerosols, especially using real-time instruments, studies to address such gap are needed to help understand the characteristics of residential aerosol particles. This is particularly important in situations when occupants are required to spend most of their time at home in a residence where indoor air quality is not routinely monitored or managed.

In this study, we assessed FAP as a surrogate for bioaerosols indoors and outdoors of an inhabited residential apartment during the COVID-19 pandemic, using the real-time UV-LIF-based WIBS. We hypothesized that FAP concentrations are higher indoors than outdoors due to increased time spent

inside during our measurement period and that the size and types of FAP that dominate inside are significantly different from those dominating outside.

Materials and methods

Study design and site description

Fig. 1 shows an overview of the study design, including the site description, data collection, data processing, and data analysis methods. Airborne particles were measured with the UV-LIF-based WIBS-5/NEO (Droplet Measurement Technologies, Longmont, CO) to characterize and quantify detected bioaerosols. Indoor and outdoor concentrations, particle sizes, and fluorescing properties were then compared. Prior to shipment and deployment, the WIBS instrument was calibrated by the manufacturer. The location of our study site and the floor plan of the assessed apartment are shown in Fig. 2a and b, respectively.

All measurements took place in a residential apartment of a multi-unit building built in 1974. The building was located about 820 ft (250 m) northward from a six-lane freeway at about 10 ft (3 m) elevation above that of the assessed apartment and about 656 ft (200 m) southward from a two-lane secondary road at about 131 ft (40 m) below the apartment level. There was a traffic light at about 250 ft (800 m) northeastward from the apartment and about 33 ft (10 m) of elevation below it. A stop sign was located about 1640 ft (500 m) northwestward from the apartment and about 148 ft (45 m) of elevation below it. Nearby, the ground was covered with grass with no flower beds or trees within 33 ft (10 m) of the building. The trees surrounding the building were deciduous, mainly maple, white ash, oak, and pear.

The apartment was a two-bedroom and two-bathroom unit with a floor area of 940 ft² (87.33 m²), two glass windows in the bedrooms, nine wooden doors (one front door, two bedroom doors, four closet doors, and two bathroom doors), and one sliding glass door in the living room that opens to a balcony. It is located on the third floor, about 33 ft (10 m) above the ground. The floor is carpeted with a 1/4 inch cut, pile-style carpet which had not been changed for at least eight years. The carpet cleaning is done as needed by simple vacuuming, with no cleaning products involved. The floor had been last vacuumed about two months prior to this study. A recirculating HVAC was present with its furnace located in the closet of the guest bedroom and the air handler filter (3M Filtrete 16 × 25 × 1) was regularly replaced at the beginning of each season or as needed. A new filter had been installed about two months prior to this study. An overhead (ceiling) fan was present in the living room and exhaust fans were present in the kitchen and both bathrooms. The use of the fans was minimized during the measurement period. When in use, the air conditioner was at 79 °F (26.11 °C) on automatic mode. Windows were kept closed during the measurement period, and door opening was minimized. There was an electric stove in the kitchen. Regarding human occupancy, two adults and two children were living in the apartment.

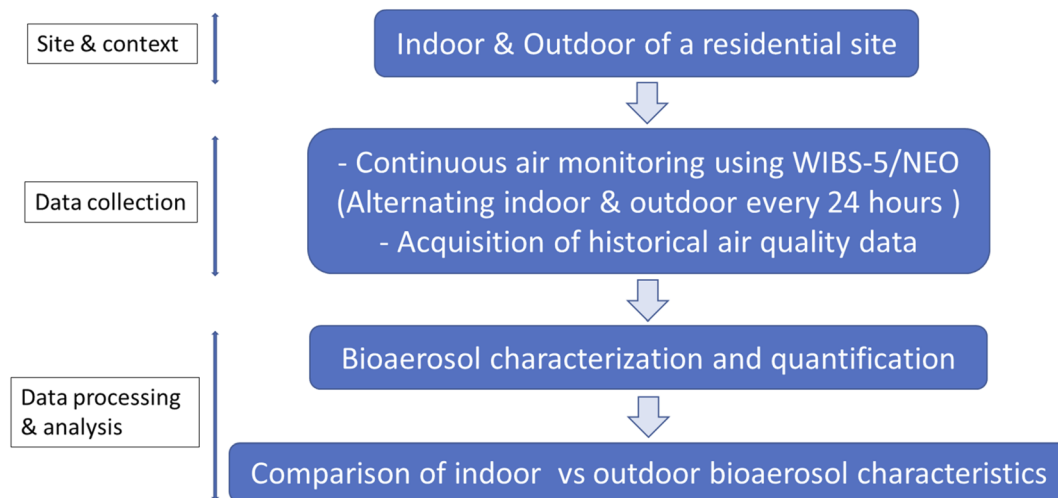


Fig. 1 Study design for assessing residential indoor and outdoor bioaerosol characteristics using the WIBS-5/NEO.

Overall, human activity patterns in the apartment can be summarized as follows. During a typical weekday, 5 AM corresponded to the residents' wake-up time, around which activities such as showers and about 10 to 20 minutes of stove and oven use for cooking breakfast took place. By 7 AM, one of the adults left for work. Lunchtime was around 11:30 AM and dinner preparation occurred between 6 PM and 7 PM. Often, three occupants were absent during dinner preparation time. For weekends, on a typical Saturday, three to four hours of cooking occurred during the morning. On a typical Sunday, the apartment was unoccupied from 9 AM to noon.

Aerosol measurement: data collection, processing, and analysis protocols

The WIBS-5/NEO is a single-particle, light scattering and fluorescence-based instrument using two UV filtered flashlamp sources optimized to excite individual particles containing tryptophan and NADH. This instrument was used to measure aerosol particles continuously for 24 hours a day, alternating indoors and outdoors every 24 hours (starting each new sampling day at midnight) from August 6 to September 30,

2020. Indoor measurements occurred in the living room. The sampling inlet tubing of the WIBS was placed at 2.5 ft (0.76 m) above the floor. This height corresponded to the breathing zone of small children. Outdoors, the sampling inlet was positioned through the crack of the sliding glass door to the balcony at the back of the building. The door crack was taped down each time to minimize air infiltration to the indoor environment.

As described in more detail in earlier studies,^{21,38,39} the WIBS light scattering was used to derive the equivalent optical diameter (EOD) of particles in the size range from 0.5 to 30 μm and the fluorescence spectroscopy measured the fluorescence of particles excited at two wavelengths. If a particle fluoresces, there are seven combinations of excitation/emission pairs. If excited at 280 nm, it can fluoresce at 310–400 nm and is labeled Type A. Similarly, when excited at 280 nm and emitting at 420–650 nm, it is labeled Type B and excited at 370 nm and emitting at 420–650 nm makes it a Type C. It is possible for a particle to fluoresce at both wavelengths when excited at 280 nm so that the seven Types A, B, C, AB, AC, BC, and ABC are analyzed.⁴⁰ The raw particle-by-particle data were averaged into five-second intervals, from which additional hourly and daily averages were calculated. The fluorescence threshold (Th) to remove the

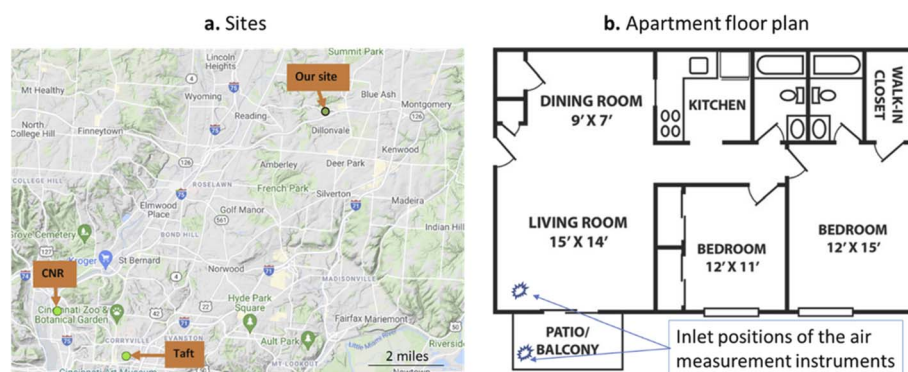


Fig. 2 (a) Map showing the location of the study site (Our site) and two air quality network monitoring stations (Cincinnati Near Road (CNR) and Taft), and (b) floor plan of our studied apartment. Distance from the study site to CNR station is 8.73 miles (14.05 km), and to Taft station is 8.40 miles (13.52 km). The study was conducted in Cincinnati, Ohio, USA.

background noise was defined as the mean forced trigger (μFT which represents the instrument background) plus 3 standard deviations (3σ) of the measurement ($\text{Th} = \mu\text{FT} \pm 3\sigma$). The volume-weighted median diameter (VWMD) was calculated by using eqn (1) with the assumption that the measured signal was proportional to the volume of the particles.

$$\text{VWMD} = \frac{\sum C_i D_i^4}{\sum C_i D_i^3} \quad (1)$$

where C_i was the number concentration of size i and D_i the diameter of size i . The number-weighted mean diameter, more sensitive to the number of particles in a size interval, was calculated as followed:

$$\text{NWMD} = \frac{\sum C_i D_i}{\sum C_i} \quad (2)$$

Temperature and relative humidity were continuously recorded with two HOBO Temp/RH logger UX100-003 devices (Onset Computer Corporation, Bourne, MA), one indoors and the other outdoors throughout the measurement period. A log was also maintained to record human activities, weather conditions and other relevant events potentially capable of influencing the measured aerosol levels.

Historical data on air pollutants

The year 2020 was atypical as it was characterized by the COVID-19 pandemic restrictions, including shutdowns of businesses and schools. During our measurement period, the restrictive measures such as shelter-in-home order and closures of businesses and schools were gradually lifted. Therefore, historical data from the Air Quality Network (AQN), which includes Southwestern Ohio Air Quality Agency and US EPA Air Quality System database, were analyzed to compare an average of the prior three years (2017–2019) of the measurement of selected air pollutants ($\text{PM}_{2.5}$, mold, and pollen), to the measurements in our study year 2020. This was done to determine if the period of our study in August–September 2020 had statistically different levels of pollutants from the previous three years (August–September 2017–2019). The AQN data included $\text{PM}_{2.5}$, mold, and pollen concentrations. The local AQN measured $\text{PM}_{2.5}$ concentrations using a real-time Microscale Thermo Sharp 5030i particulate monitor (Thermo Scientific, Waltham, MA) to record one-minute-resolution data at the Cincinnati Near Road (CNR) station (8.73 miles (14.05 km) from the study site) (Fig. 2a). Pollen and mold were measured at the Taft station (located 8.40 miles (13.52 km) from the studied site) (Fig. 2a) using a Rotorod sampler (Aerobiology Research Laboratories, Ottawa, Ontario) to collect one-minute air samples every 10 minutes for roughly 24 hours every weekday.

Statistical analysis

The WIBS' particle-by-particle and second-by-second raw data were pre-processed to obtain 5 minute resolution data, which were further processed to hourly and daily averaged data. We then analyzed the trends of daily and aggregate hourly mean

concentrations (average concentrations of all measurement days for each hour (0–23 hours)). Indoor and outdoor particle number concentrations were compared using the Wilcoxon rank sum test (with two variables) and the Kruskal–Wallis test (with more than two variables). The Spearman's rank test was used for the correlation between TAP and TFAP. The significance of the mean rank difference between indoor and outdoor particle diameter was tested using the unpaired t -test with equal variance for all particle types. We also performed the Wilcoxon rank sum test to compare the historical air quality data from 2017–2019 to the year 2020 data corresponding to our WIBS measurement period. The statistical testing was conducted using RStudio version 1.1.463 (run on R statistical software version 4.1.1) at a significance level of $\alpha = 0.05$.

Results

Comparison of indoor and outdoor TAP, TFAP, and NFAP

The overall descriptive statistics, mean, median, standard error (SE), and standard deviation (SD) of aerosol particle concentrations, temperature, and relative humidity data are presented in Table 1. The comparison of particle number concentrations indicates that the mean \pm SE ($4.14 \pm 0.38 \text{ cm}^{-3}$) of the indoor daily TAP concentrations was significantly higher ($p < 0.001$) than the outdoor mean ($2.16 \pm 0.15 \text{ cm}^{-3}$) (Table 1; Fig. 3a). A similar result was found for TFAP: the mean ($0.98 \pm 0.09 \text{ cm}^{-3}$) of indoor daily TFAP concentrations was significantly higher ($p < 0.001$) than the outdoor mean ($0.39 \pm 0.02 \text{ cm}^{-3}$) (Table 1; Fig. 3b). Likewise, for non-fluorescent aerosol particles (NFAP), the indoor mean ($3.16 \pm 0.30 \text{ cm}^{-3}$) was significantly higher ($p < 0.001$) than the outdoor mean ($1.77 \pm 0.13 \text{ cm}^{-3}$) (Table 1; Fig. 3c).

The time series of daily mean concentrations in Fig. 4a–c show similar patterns over time for indoor TAP, TFAP and NFAP concentrations, *i.e.*, the peaks and troughs observed in indoor TAP, TFAP and NFAP concentrations coincided in time. The same was observed with their corresponding outdoor mean concentrations, except that the variation in outdoor mean concentrations was lower compared to indoors. Spearman's rank correlation test between TAP and TFAP concentrations resulted in significant ($p < 0.001$) correlation coefficients of 0.92 indoors and 0.81 outdoors, suggesting a positive relationship. Also, no clear differences were observed between weekdays and weekends.

Particle concentrations vary throughout the day, trends that were captured with the aggregate hourly mean concentrations. Indoors, maxima were observed at around 7 AM and 11 AM for TAP and TFAP (Fig. 5a and b). Outdoors, the highest concentrations were observed around 10 PM for both the TAP and the TFAP, but much less pronounced with the latter (Fig. 5b). The NFAP concentrations presented the same trends as the TAP concentrations (Fig. 5c).

In comparing indoor and outdoor TFAP fractions (TFAP/TAP), Fig. 6a shows that the mean \pm SE fraction indoors ($23.22 \pm 0.77\%$) was significantly higher than outdoors ($19.37 \pm 0.72\%$), because of the significant difference in the mean ranks. The time series (Fig. 6b) shows that TFAP fraction presented

Table 1 Overall descriptive statistics: Mean, median standard error (SE) and standard deviation (SD) of the indoor and outdoor particle concentrations, temperature, and relative humidity between August 6 and September 30, 2020^a

	Indoors (<i>N</i> = 24 days)				Outdoors (<i>N</i> = 26 days)			
	Mean	Median	SE	SD	Mean	Median	SE	SD
WIBS: daily particle number concentration and fluorescent particle fraction								
TAP (cm ⁻³)	4.14	3.44	0.38	1.86	2.16	2.12	0.15	0.74
TFAP (cm ⁻³)	0.98	0.79	0.09	0.43	0.39	0.37	0.02	0.12
NFAP (cm ⁻³)	3.16	2.56	0.30	1.45	1.77	1.82	0.13	0.65
FAP fraction (%)	23.22	22.49	0.77	3.77	19.37	19.25	0.72	3.65
HOBO: temperature and relative humidity								
Temperature (°F)	78.35	78.68	0.19	0.96	69.20	70.94	2.40	12.23
Relative humidity (%)	47.39	47.06	0.41	2.09	74.72	77.26	1.42	7.24

^a TAP = total aerosol particles, TFAP = total fluorescent aerosol particles, NFAP = non-fluorescent aerosol particles, FAP = fluorescent aerosol particles.

more variability indoors compared to outdoors, as confirmed by the difference in the indoor and outdoor ranges (Fig. 6a).

Comparison of indoor and outdoor FAP types

The FAP detected by the WIBS were a mixture of different groups of particles that can be discriminated based on their fluorescence emission wavelengths. Here, we considered the seven derived FAP types A, B, C, AB, AC, BC and ABC as defined by Perring *et al.*, who used the WIBS-4,⁴⁰ to investigate which FAP types were more prevalent in the indoor and outdoor environments. The WIBS-4 does not differ from WIBS-5 in this regard. For both indoors and outdoors, the Kruskal–Wallis test indicated that the mean ranks of concentrations of at least one of the FAP types was significantly different from the others ($p < 0.001$). As illustrated in Fig. 7, the FAP type A dominated indoors, followed by the types BC, B, C, ABC, AB, and AC. Outdoors, the mean number concentrations of types B, ABC, and BC were the highest, followed by A, C, AB, and AC. Moreover, except for type ABC, all other types had higher concentrations indoors compared to outdoors. This difference was significant for all particle types, except B.

Volume and number concentration size distributions of TFAP

Aggregate data on hourly averages allowed us to assess the temporal trends of the size distributions of the TFAP. The resulting heat maps suggest that the highest volume concentrations corresponded to TFAP, with EOD ranging 1–2.5 μm indoors (Fig. 8a) and 2–4 μm outdoors (Fig. 8b). The descriptive statistics (mean \pm SE) of all hourly volume-weighted median diameters of TFAP were 1.66 ± 0.01 μm indoors and 2.07 ± 0.01 μm outdoors. The highest peaks occurred at 1.72 μm and 2.12 μm indoors and outdoors, respectively (Fig. 9a). Hourly number-weighted mean diameters of the TFAP were 1.38 ± 0.01 μm indoors and 1.75 ± 0.01 μm outdoors. The highest peaks occurred at the particle size of 1.4 μm and 1.90 μm indoors and outdoors, respectively (Fig. 9b). We also used the aggregate data on hourly averages of all particle types to calculate the mean particle diameters based both on number concentrations (Table 2) and volume concentrations (Table 3). For each particle type, the outdoor mean diameter weighted by the number concentration was significantly higher outdoors than indoors ($p < 0.001$). Similar results were seen with the mean diameter weighted by the volume concentration (Table 3) with the

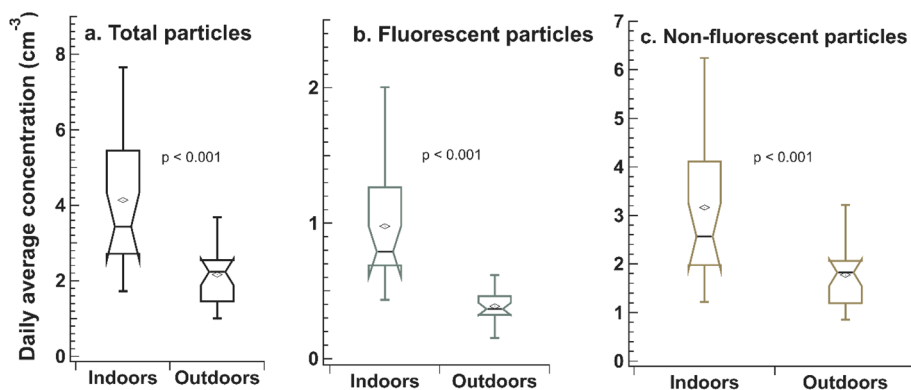


Fig. 3 Comparison of the indoor (*N* = 24) and outdoor (*N* = 26) daily average concentrations of (a) total aerosol particles, (b) total fluorescent aerosol particles and (c) non-fluorescent particles, measured with the WIBS. On each boxplot, the horizontal bars indicate the minimum, first quartile, median (at the notch), third quartile, and maximum, and the diamond symbol represents the mean; *p* is the *p*-value of Wilcoxon rank sum test at a significance level $\alpha = 0.05$.

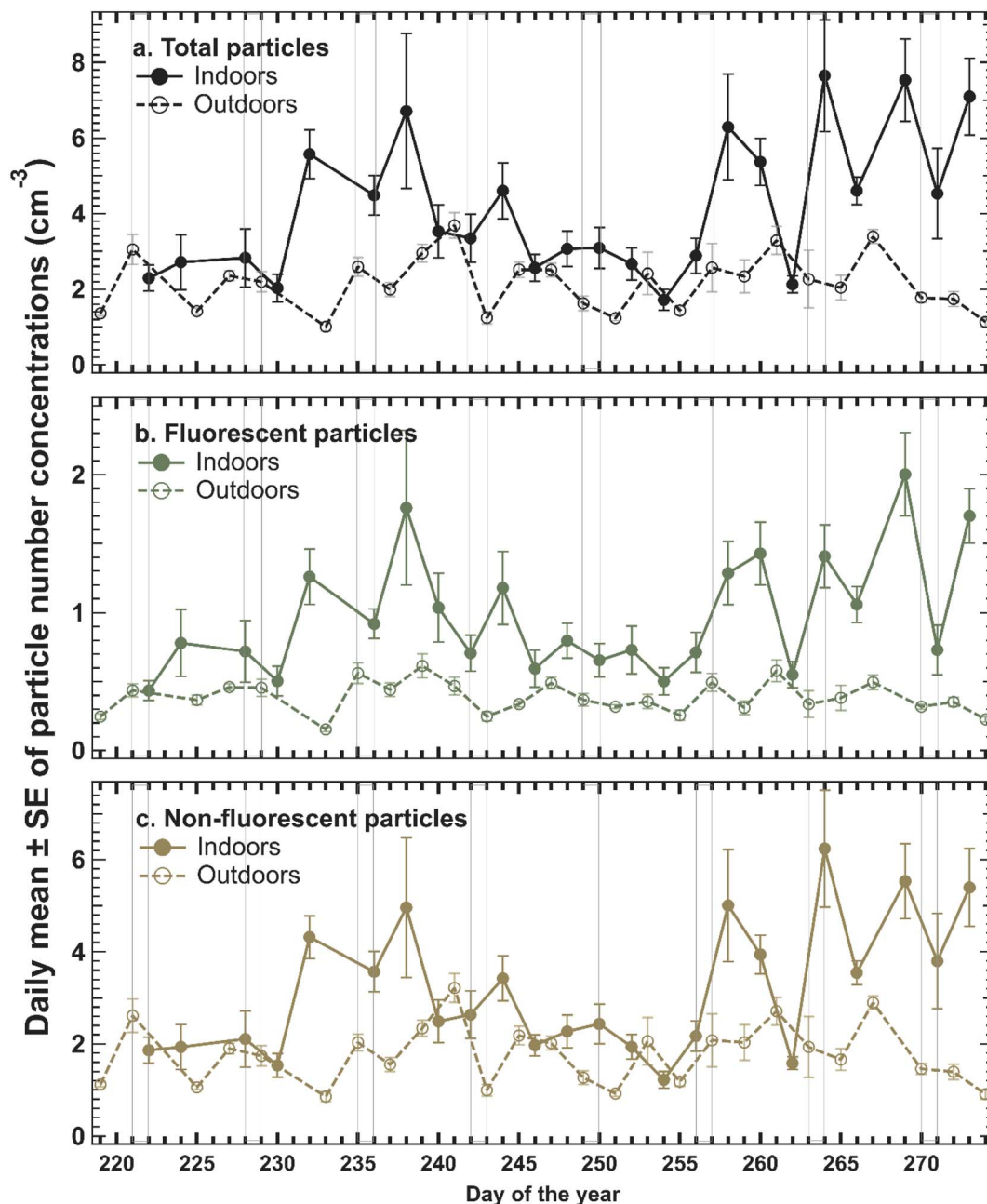


Fig. 4 Time series showing the patterns of the indoor ($N = 24$) and outdoor ($N = 26$) daily mean concentrations of (a) total aerosol particles, (b) total fluorescent aerosol particles and (c) non-fluorescent aerosol particles, measured with the WIBS. The capped vertical line at each data point maker represents the standard error of the mean. The vertical grey bars in the plot indicate weekend days.

exception of the FAP type A, for which the difference was not significant ($p = 0.694$).

Historical air quality data

For each of the selected pollutants ($PM_{2.5}$, mold, and pollen), we compared the average concentrations of the prior three years 2017, 2018, and 2019 with the average concentrations of the year 2020, using only the data corresponding to our measurement period (from August 6 through the end of September). There were no significant differences ($p > 0.05$) in the averages of $PM_{2.5}$, mold, and pollen over the prior three years 2017–2019

($12.4 \pm 3.2 \mu\text{g m}^{-3}$, 2568 ± 950 spores per m^3 , and 50 ± 47 grains per m^3 , respectively) compared to the year 2020 ($11.2 \pm 3.8 \mu\text{g m}^{-3}$, 1780 ± 1012 spores per m^3 and 79 ± 78 grains per m^3 , respectively) (Fig. 10a–c).

Discussion

This study highlights the indoor and outdoor comparison of number concentrations and size distributions of aerosol particles measured with the real-time UV-LIF-based WIBS instrument. Measurements were taken during the COVID-19

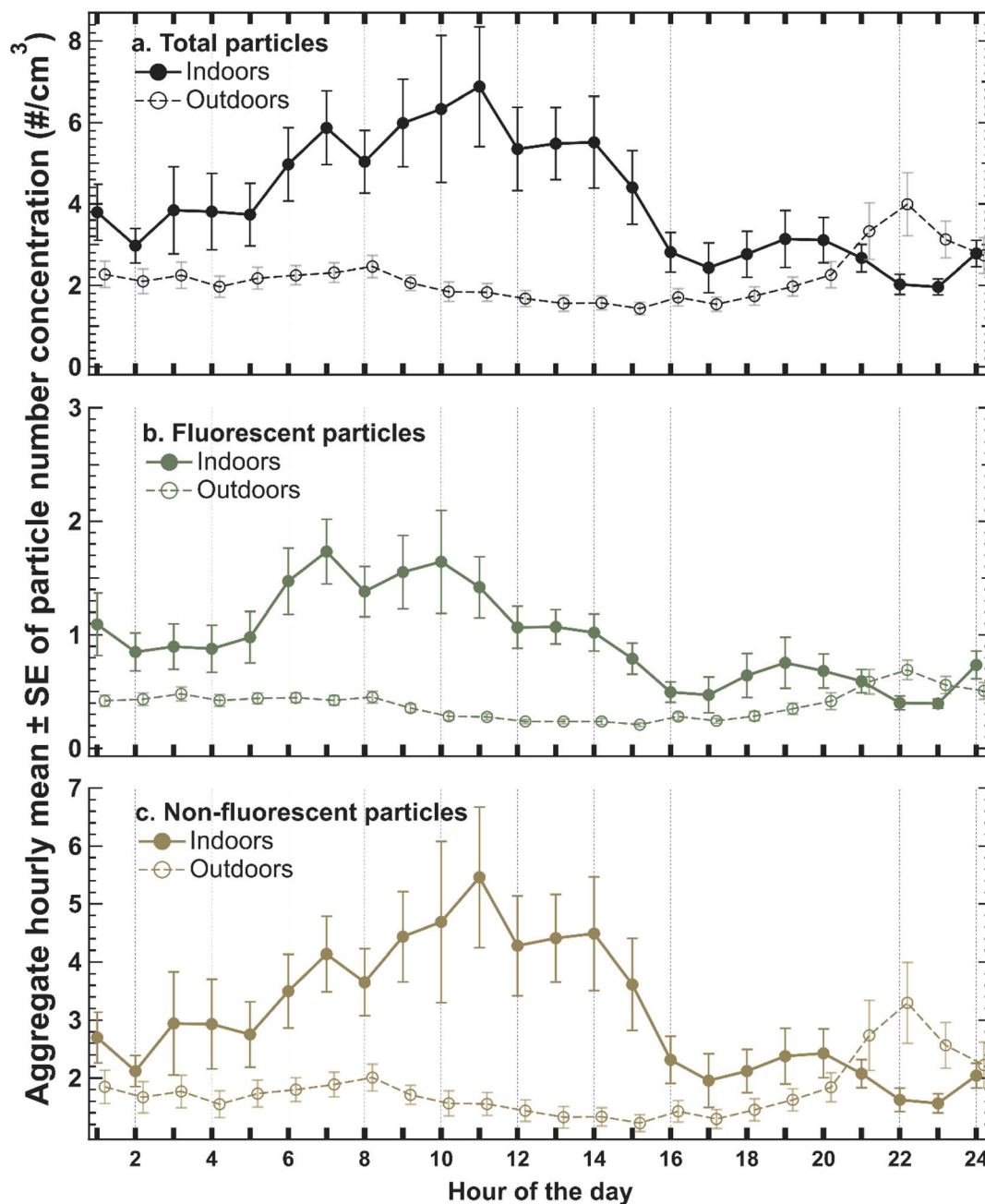


Fig. 5 Pattern comparison of indoor and outdoor aggregate hourly mean concentrations ($N = 24$) of the (a) total aerosol particles, (b) the total fluorescent aerosol particles and (c) non-fluorescent aerosol particles, measured with the WIBS. The capped vertical line at each data point marker represents the standard error of the mean.

pandemic. While the State stay-at-home order date was known (March 26, 2020), the reopening of businesses and schools happened rather gradually. Moreover, after the reopening, some people continued to study and work from home.

Indoor-outdoor comparison of TAP, TFAP, and NFAP

We found that the mean ranks of the number concentrations of TAP, TFAP, and NFAP were significantly higher indoors than outdoors. This was expected as the occupants of the apartment continued to work and attend school from home. The higher

particle concentrations indoors compared to outdoors were likely due to various human activities that generate and/or resuspend bioparticles such as bacteria and fungi.^{35,36} We also found that the daily averages of the concentrations of TFAP followed the same pattern as the TAP both indoors and outdoors. This parallel trend was confirmed with a strong positive correlation between the TAP and TFAP concentrations. These results point towards common sources for TAP and TFAP. These sources were most likely due to human activities. Human occupancy-related factors that could contribute to the increased

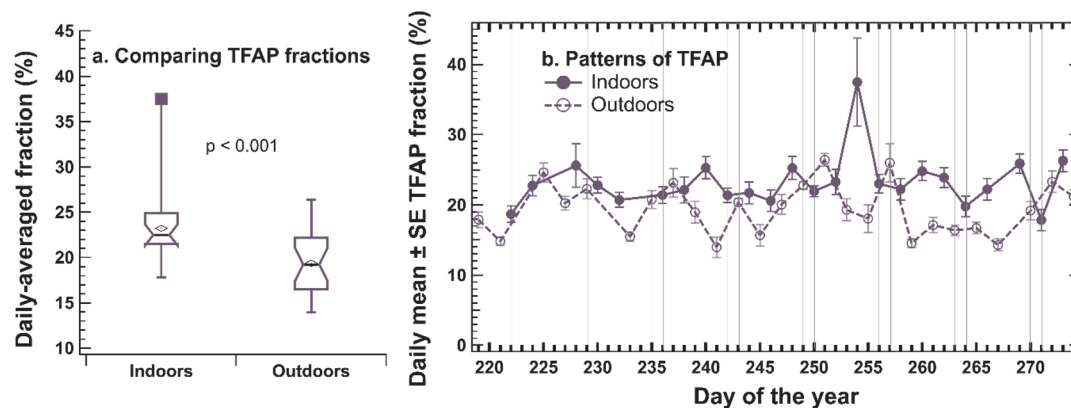


Fig. 6 Indoor ($N = 24$) and outdoor ($N = 26$) daily mean of total fluorescent aerosol particle fractions: (a) boxplot comparing fractions and (b) time series showing the daily fraction patterns. In each boxplot, the horizontal bars indicate the minimum, first quartile, median (at the notch), third quartile, and maximum, and the diamond symbol represents the mean. The square data point represents an outlier. Outliers are points outside the inner fences, with inner fences = third quartile + $1.5 \times \text{IQR}$ and first quartile $- 1.5 \times \text{IQR}$ (with IQR being the interquartile range). In the time series plot, the capped vertical lines at each data point marker represent the standard error of the mean. The vertical bars show weekend days. The p -value shows the result of Wilcoxon rank sum test at a significance level $\alpha = 0.05$.

particle concentrations in our study include particle shedding from the occupants' skins, clothing and furniture, particle resuspension from the carpeted flooring caused by walking, and particle generation from cooking activities. Indeed, Li *et al.*,³⁵ who recently used the WIBS instrument to monitor indoor and outdoor air of a naturally ventilated bedroom, reported elevated indoor bioaerosol concentrations when the assessed room was occupied. Studies, such as those conducted in classrooms by Hospodsky *et al.*²⁸ and Qian *et al.*,⁴¹ and in a living laboratory office by Patra *et al.*,⁴² corroborate our interpretation that human occupancy represented a major contributor to elevated indoor bioaerosol concentrations. More recently, Nieto-Caballero *et al.*³⁷ conducted fluorescent aerosol cytometry in classrooms using the InstaScope (DetectionTek, Boulder, CO,

USA), a direct-reading instrument operationally similar to the WIBS, and reported higher bioaerosol concentrations indoors than outdoors. Nathu *et al.*³⁶ also used an InstaScope to characterize concentrations and types of bioaerosols during common human activities that take place when home health-care workers are providing care in their patients' homes. They reported that human activities like walking, vacuuming, showering, and cooking contribute to an increase in the concentrations of fluorescent particles. Other previous studies have reported similar findings, although the techniques used were different. For example, Tian and collaborators³¹ used a fluorescence-based ultraviolet aerodynamic particle sizer (UV-APS) to measure fluorescent bioaerosol and TAP in the kitchen/dining area of residences. They found that occupant activities

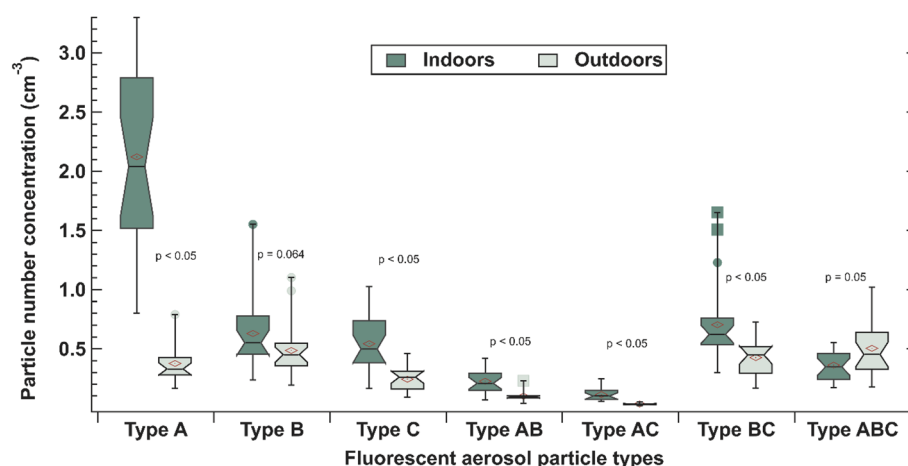


Fig. 7 Boxplot comparing the concentrations of fluorescent particle types indoors ($N = 24$) versus outdoors ($N = 26$). On a boxplot, the horizontal bars indicate the minimum, first quartile, median (at the notch), third quartile, and maximum, and the diamond symbol represents the mean. Green circle and green square data points represent outliers and far outliers, respectively. "Outliers" are points outside the inner fences and "far outliers" are points beyond the outer fences, with inner fences = third quartile + $1.5 \times \text{IQR}$ and first quartile $- 1.5 \times \text{IQR}$, and outer fences = third quartile + $3 \times \text{IQR}$ and first quartile $- 3 \times \text{IQR}$ (with IQR being the interquartile range). The p -value shows the result of Wilcoxon rank sum test at a significance level $\alpha = 0.05$.

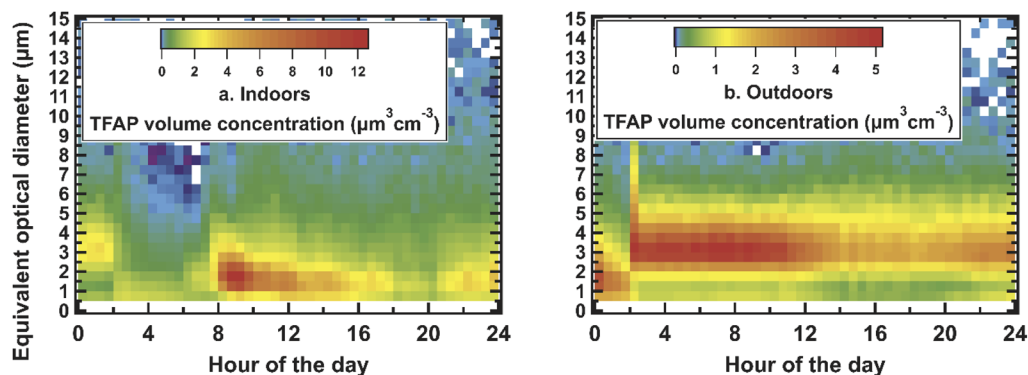


Fig. 8 Spectral size distribution of hourly averages of the total fluorescent aerosol particles (TFAP) with the color scale based on the particle volume concentration ($\mu\text{m}^3 \text{cm}^{-3}$): (a) indoors and (b) outdoors.

(walking, vacuuming, and cooking) strongly influenced indoor fluorescent bioaerosol concentrations, which were an order of magnitude higher in the occupied compared to the vacant house. Using a single-stage Andersen sampler and settling plates, Faridi *et al.*⁴³ measured the concentrations of bacterial and fungal bioaerosols in a retirement home and a school dormitory and found that the indoor concentrations were higher than those outdoors. In another study that evaluated bioaerosols indoors and outdoors of a university classroom using rDNA sequencing, Qian and collaborators⁴⁴ also reported higher indoor bioaerosol levels consistent with human occupancy.

In some previous studies, higher outdoor concentrations compared to indoor levels have been reported. Lee *et al.*⁴⁵ used Button Inhalable Aerosol Samplers combined with microscopic counting to measure concentrations of pollen and fungal spores in homes in Cincinnati, Ohio. Contrary to our findings, they reported higher concentrations outdoors than indoors. The different results could be due to methodological differences. The study by Lee *et al.*⁴⁵ did not include bacteria, which can have a substantial contribution to indoor bioaerosol concentrations in occupied spaces. Li *et al.*,³⁵ who used the same method as ours, reported higher median concentrations outdoors

compared to indoors for all seven FAP types. This is an opposite trend compared to our finding that the fluorescent particle concentrations were greater indoors than outdoors. Li *et al.*³⁵ reported median concentrations (with IQR) of 0.7 (0.5) and 1.4 (0.7) cm^{-3} for TFAP in indoor and outdoor environments, respectively. Our mean number concentrations of the TAP and TFAP indoors were higher than those reported by Li *et al.* with the differences being 2.48 and 12%, respectively. The difference between indoor and outdoor NFAP was only -0.16% . The difference between TAP and TFAP could be explained by the fact that in our study, the residents of the assessed apartment spent a longer time inside due to pandemic-related precautions, which consequently increased human activities. Outdoors, our mean number concentrations for TAP, NTAP, and TFAP were lower; the difference was -58% for each, respectively. The differences in percentage were calculated by the following formula: $100 \times (\text{median number concentrations reported by Li } et al. - \text{our median number concentration}) / \text{median number concentrations reported by Li } et al.$ The large difference observed outdoors can be due to poor ambient air quality in Singapore in 2019 when particulate matter levels were reported to be the highest during the recent period of 2015–2020.⁴⁶ Li's study³⁵ took place in a naturally ventilated bedroom on the 6th

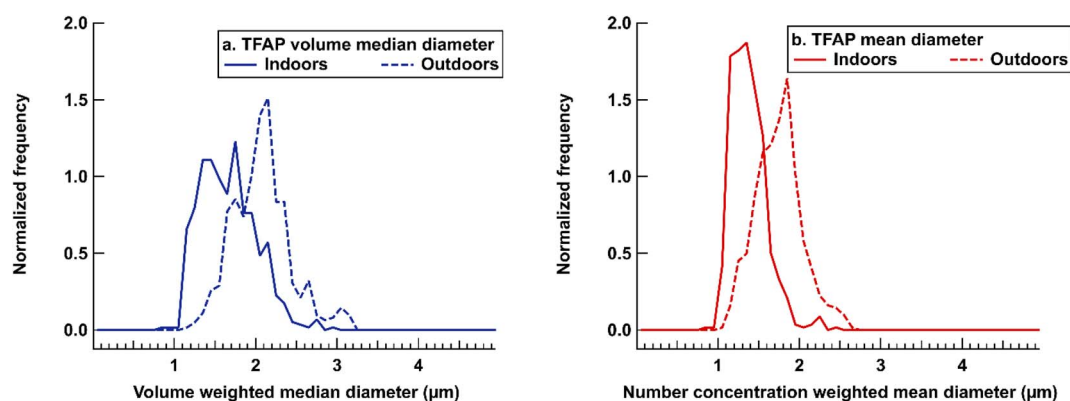


Fig. 9 Size distribution histograms of total fluorescent particle based on (a) volume weighted median diameter and (b) number concentration weighted mean diameter.

Table 2 Mean, median, standard error (SE), and standard deviation (SD) of number weighted particle diameters (NWMD) in μm based on hourly-averaged number concentrations indoors ($N = 580$) versus outdoors ($N = 624$) for all particle types, and p -values from unpaired t -test results^a

Particle type	Indoor NWMD (μm)				Outdoor NWMD (μm)				Unpaired t -test
	Mean	Median	SE	SD	Mean	Median	SE	SD	p -Value
TAP	1.07	1.04	0.00	0.09	1.18	1.15	0.01	0.12	<0.001
TFAP	1.38	1.35	0.01	0.22	1.74	1.75	0.01	0.29	<0.001
FAP types									
A	1.27	1.26	0.01	0.13	1.32	1.26	0.01	0.13	<0.001
B	1.04	1.02	0.00	0.06	1.14	1.26	0.00	0.10	<0.001
C	1.11	1.08	0.01	0.11	1.41	1.08	0.01	0.26	<0.001
AB	1.63	1.59	0.01	0.31	1.70	1.59	0.01	0.27	<0.001
AC	1.68	1.66	0.01	0.22	1.99	1.66	0.01	0.29	<0.001
BC	1.29	1.26	0.01	0.15	1.60	1.26	0.01	0.25	<0.001
ABC	2.51	2.56	0.02	0.40	2.79	2.56	0.01	0.28	<0.001

^a TAP = total aerosol particles, TFAP = total fluorescent aerosol particles, FAP = fluorescent aerosol particles.

floor of a residential building, and outdoor inlet level can be estimated to be at least about 66 ft (20 m) above the ground, meaning that elevation does not explain the difference. Also, Singapore's high population density combined with its tropical high outdoor temperature and relative humidity, (with respective annual means being 79.9 °F (26.6 °C) and 84%) could have played a role.⁴⁷

The patterns of aggregate hourly averages were also similar for TAP and TFAP. The peaks observed around 7 AM and 11 AM indoors can be explained by increased human activities, such as walking and crawling, that likely contributed to resuspending settled particles from the carpet and enhanced particle shedding from furniture, clothes, and skin, as well as emissions from cooking activities.^{28,44,48–54} The first peak at 7 AM corresponds to the morning time when the apartment occupants were most actively moving around, while 11 AM corresponds to the time of cooking and eating lunch. Tian *et al.* (2018) emphasized the role of cooking activities, such as emissions from burning stove plates, liquid boiling, and tap water running in increasing TFAP concentrations.³¹ We found that aggregate

hourly patterns outdoors had peak concentrations of TAP, TFAP, and NFAP around 10 PM. This is supported by studies that reported maximal release of fungal spores and pollen during nighttime, mainly due to an increase in the relative humidity^{55–57} and the decrease in the atmospheric boundary layer height during nighttime.^{58,59}

Aerosols detected by the WIBS were a mixture of fluorescent and non-fluorescent particles. Our study focused on FAP as a surrogate for total bioaerosols. The proportions they represented, relative to the TAP detected by the WIBS both indoors and outdoors, offer valuable information since they are more likely to contain most of the bioaerosols. In this study, the TFAP fractions were about 24% indoors and 19% outdoors. This indicates that TFAPs were relatively more abundant indoors than outdoors. The TFAP fractions in the current study were in accordance with Li *et al.*,³⁵ who reported median (\pm interquartile range) bioaerosol fractions of $19 \pm 5\%$ indoors and $17 \pm 3\%$ outdoors. Additionally, Calvo *et al.* reported a range of 15–35% for the TFAP fraction of outdoor particles with the size

Table 3 Mean, median, standard error (SE), and standard deviation (SD) of hourly-averaged volume weighted median diameter (VWMD) in μm , indoors ($N = 580$) versus outdoors ($N = 624$) for all particle types, and p -values from unpaired t -test results^a

Particle type	Indoor VWMD (μm)				Outdoor VWMD (μm)				Unpaired t -test
	Mean	Median	SE	SD	Mean	Median	SE	SD	p -Value
TAP	1.48	1.45	0.01	0.30	1.85	1.82	0.01	0.35	<0.001
TFAP	1.66	1.65	0.01	0.34	2.07	2.06	0.01	0.35	<0.001
FAP types									
A	1.35	1.31	0.01	0.19	1.34	1.33	0.01	0.14	0.694
B	1.05	1.03	0.00	0.06	1.16	1.14	0.01	0.11	<0.001
C	1.12	1.09	0.01	0.12	1.43	1.42	0.01	0.26	<0.001
AB	1.65	1.60	0.01	0.32	1.71	1.70	0.01	0.27	<0.001
AC	1.68	1.66	0.01	0.23	2.00	1.99	0.01	0.29	<0.001
BC	1.32	1.29	0.01	0.17	1.65	1.64	0.01	0.25	<0.001
ABC	2.58	2.63	0.02	0.41	2.87	2.90	0.01	0.29	<0.001

^a TAP = total aerosol particles, TFAP = total fluorescent aerosol particles, FAP = fluorescent aerosol particles.

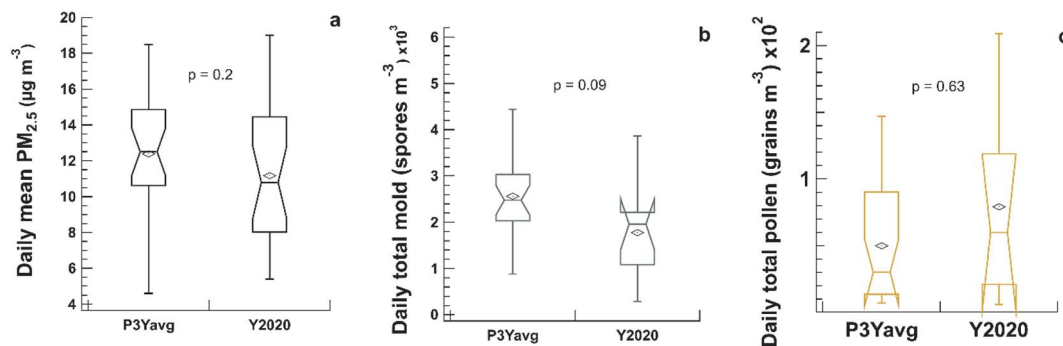


Fig. 10 Comparison of the average of the historical air quality data for the prior three years from 2017 to 2019 (P3Yavg) with the year 2020 (Y2020) for the daily concentrations of (a) $\text{PM}_{2.5}$, (b) mold, and (c) pollen. Only data corresponding to the measurement period from August through September were included ($N = 50$). On a boxplot, the horizontal bars indicate the minimum, first quartile, median (at the notch), third quartile, and maximum, and the diamond symbol represents the mean; p is the p -value of Wilcoxon rank sum test at a significance level $\alpha = 0.05$.

above $2\ \mu\text{m}$;⁶⁰ and researchers in other studies have found similar fractions as well.^{20,61,62}

Comparison of indoor and outdoor fluorescent aerosol types

Based on the fluorescence threshold setting, emission intensity, and emission bands, the FAP were categorized into seven types A, B, C, AB, AC, BC, and ABC.^{39,40} In this study, we found that the FAP type A dominated indoors while types B, BC, and ABC dominated outdoors. In contrast, in the study by Li *et al.*, type B dominated both indoors and outdoors.³⁵ Using the chamber catalogs of optical and fluorescent signatures diagram published by Hernandez *et al.*, the fluorescence types can be grouped broadly into bacteria-, fungi-, and pollen-like fluorescing particles.⁶³ Type A particles, which dominated indoors in our study, are mostly bacteria. Among the dominant types outdoors, type B particles are mostly fungi, while types BC and ABC are mostly pollen.⁶³ In our study, FAP type ABC was the only FAP type that was higher outdoors than indoors. This is in agreement with Lee *et al.*, who concluded that only a small fraction of outdoor pollen penetrates into indoor environments.⁴⁵ Obviously, the different FAP types behave differently, and the high level of bacteria indoors would have been generated mostly by humans.^{51,64,65} In fact, in Li *et al.*'s study, human occupancy and activities were simulated by only one person being present intermittently,³⁵ whereas the apartment in which we took our measurements was almost always occupied by three or four inhabitants due to the ongoing pandemic precautions although State restrictions were relaxed. This quasi-permanent human occupancy and activities in our study could have substantially contributed to the dominance of bacteria indoors.^{28,66,67} It appears that in the absence of bacteria and pollen, fungi dominated both indoors and outdoors in the study of Li *et al.*³⁵

Size distributions of the total fluorescent aerosol particles

The WIBS can detect particles in the size range of $0.5\text{--}30\ \mu\text{m}$. In our study, the size of the detected FAP varied between 0.5 to $15\ \mu\text{m}$ both indoors and outdoors, with particles $>15\ \mu\text{m}$ being negligible. For the TFAP sizes, we found that the mean of the

volume-weighted median diameters was $1.67\ \mu\text{m}$ indoors and $2.09\ \mu\text{m}$ outdoors. The quasi totality of our TFAP were of size below $2.5\ \mu\text{m}$, whereas Li *et al.* reported that TFAP with size $>2\ \mu\text{m}$ dominated indoors and those with size $>3.5\ \mu\text{m}$ dominated outdoors.³⁵ This difference could be due to the specificity of each study site and also differences in the geographical region. However, our study found that the majority of the FAP were in the size range of fine particles ($<2.5\ \mu\text{m}$). From a health perspective, fine particles pose more threats than coarser particles as they can reach deep into the lung, interact with the alveoli, and therefore can potentially cause serious respiratory and cardiovascular adverse effects.⁶⁸

Comparison of the historical levels of $\text{PM}_{2.5}$, mold, and pollen

We also investigated whether the data obtained were anomalies or representative of the air quality trend across multiple years in the monitoring area, given the unusual change in human behavior and activity patterns due to the COVID-19 pandemic restrictions, including shutdowns of businesses and schools during the year 2020. Indeed, several studies have shown decreased outdoor air pollution in various regions around the globe during the pandemic.^{32,69–81} As our historical air quality data showed, the differences in the average concentrations of $\text{PM}_{2.5}$, mold, and pollen outdoors between the prior three years, 2017–2019, and the year 2020 were not significant. This suggests that our outdoor measurements from August 6 through September 30 were typical and representative of the ambient air quality in the area over the last four years.

Limitations, strengths, and future research

The measurements in the study were taken in only one residential apartment and during the summer season only. As such, our findings at this stage may not be generalized. It is worth noting that using TFAP concentrations as a surrogate for bio-aerosol concentration should be taken with caution due to potential fluorescence interference issues. It is challenging to absolutely and exclusively discriminate bioparticles since other fluorescent particles of non-biological origin could also fluoresce following the excitation with the same wavelengths. This

can overestimate the actual bioaerosol concentrations. Such potential interferences could be humic-like substances, secondary organic particles, mineral dust, polycyclic aromatic hydrocarbons, and soot.^{23,31} The risk of underestimation of bioaerosols is also possible because WIBS-5 can detect particles ranging from 0.5 μm to 30 μm in size. Consequently, bio-particles outside these detection limits cannot be measured.

The strength of this study resides in its uniqueness of the real-time assessment of residential aerosol particles both indoors and outdoors using the WIBS, a cutting-edge UV-LIF instrument. Furthermore, the study was conducted during the 2020 COVID-19 pandemic restrictions period. Comparing historical 2017–2019 air quality data to the year 2020 ensures that the ambient air quality was representative of the time and the area. To our knowledge, no other study has yet assessed and compared residential indoor and outdoor bioaerosols concurrently during the COVID-19 pandemic using a real-time UV-LIF-based method.

This current study can pave the way for future, more extended research studies to assess a broader range of bioaerosols to evaluate personal exposure to those bioaerosols in residential settings. It also will serve as a baseline in investigating the association between such exposures and potential health outcomes. In fact, this study is part of a larger project that aims to evaluate hazardous exposures in residential settings.

Conclusion

In the present study, we assessed FAP as a proxy for bioaerosols both indoors and outdoors at a residential site using the WIBS, a real-time, UV-LIF-based single-particle optical spectrometer. We found that indoor environments can be highly contaminated with airborne biological particles, human activities being a major contributor. The results indicate the potential for high exposure to FAP in the fine particle size range and consequent adverse health effects. The direct-reading WIBS has the advantage of capturing almost instantaneously variations in particle concentrations over time. Therefore, we recommend this novel tool for time- and size-resolved monitoring of FAP. This study will contribute to filling the gap in understanding the interplay between indoor and outdoor bioaerosol particles in residential environments. It will also serve as a preliminary database for future exposure assessment studies in residential environments, to help improve air quality in these environments for the protection of people's health.

Author contributions

Conceptualization, Yao S. Addor, Tiina Reponen, and Nicholas Newman; methodology, Yao S. Addor, Tiina Reponen, and Roman Jandarov; software, commercially available Igor Pro 8 and 9, and open-source RStudio version 1.1.463; validation, Tiina Reponen, Nicholas Newman, and Darrel Baumgardner; formal analysis, Yao Addor and Roman Jandarov; investigation, Yao S. Addor and Tiina Reponen; resources, Tiina Reponen, Nicholas Newman, and Yao S. Addor; data curation, Darrel

Baumgardner, Dagen Hughes, and Yao S. Addor; writing—original draft preparation, Yao Addor; writing—review and editing, Yao S. Addor, Tiina Reponen, Darrel Baumgardner, Nicholas Newman, Roman Jandarov, and Dagen Hughes; visualization, Yao S. Addor; supervision, project administration, and funding acquisition, Tiina Reponen. All authors have read and agreed to the published version of the manuscript.

Conflicts of interest

There are no conflicts to declare.

Acknowledgements

This research study was supported by the National Institute for Occupational Safety and Health through the Targeted Research Training (TRT) Program of the University of Cincinnati Education and Research Center Grant #T42OH008432. We thank Droplet Measurement Technologies (DMT, Longmont, CO) for providing us with the WIBS-5/NEO and for helping with the data processing, and the Southwestern Ohio Air Quality Agency (AQA) for providing us with the air pollution data and for referring us to other useful resources. We also thank the dwellers of the assessed apartment for having accepted the burden of the measurement process.

References

- 1 J. Douwes, P. Thorne, N. Pearce and D. Heederik, Bioaerosol Health Effects and Exposure Assessment: Progress and Prospects, *Ann. Work Exposures Health*, 2003, **47**(3), 187–200.
- 2 U. Pöschl, Atmospheric Aerosols: Composition, Transformation, Climate and Health Effects, *Angew. Chem., Int. Ed.*, 2005, **44**(46), 7520–7540.
- 3 V. Després, J. A. Huffman, S. M. Burrows, C. Hoose, A. Safatov, G. Buryak, *et al.*, Primary biological aerosol particles in the atmosphere: a review, *Tellus B*, 2012, **64**, 15598.
- 4 D. G. Georgakopoulos, V. Després, J. Fröhlich-Nowoisky, R. Psenner, P. A. Ariya, M. Pósfai, *et al.*, Microbiology and atmospheric processes: Biological, physical and chemical characterization of aerosol particles, *Biogeosciences*, 2009, **6**, 721–737.
- 5 T. Reponen, J. Lockey, D. I. Bernstein, S. J. Vesper, L. Levin, M. D. Khurana Hershey, G. K. PhD, *et al.*, Infant origins of childhood asthma associated with specific molds, *J. Allergy Clin. Immunol.*, 2012, **130**, 639–644.
- 6 J. Madureira, I. Paciência, J. Rufo, E. Ramos, H. Barros, J. P. Teixeira, *et al.*, Indoor air quality in schools and its relationship with children's respiratory symptoms, *Atmos. Environ.*, 2015, **118**, 145–156.
- 7 M. Jahangiri, M. Neghab, G. Nasiri, M. Aghabeigi, V. Khademian, R. Rostami, *et al.*, Respiratory disorders associated with occupational inhalational exposure to bioaerosols among wastewater treatment workers of petrochemical complexes, *J. Occup. Environ. Med.*, 2015, **6**, 41–49.

- 8 W. W. Nazaroff, Indoor bioaerosol dynamics, *Indoor Air*, 2016, **26**(1), 61–78.
- 9 K.-H. Kim, E. Kabir and S. A. Jahan, Airborne bioaerosols and their impact on human health, *J. Environ. Sci.*, 2018, **67**, 23–35.
- 10 A. P. Verhoeff and H. A. Burge, Health Risk Assessment of Fungi in Home Environments, *Ann. Allergy, Asthma, Immunol.*, 1997, **78**, 544–556.
- 11 M. A. Ross, L. Curtis, P. A. Scheff, D. O. Hryhorczuk, V. Ramakrishnan, R. A. Wadden, *et al.*, Association of asthma symptoms and severity with indoor bioaerosols, *Allergy*, 2000, **55**, 705–711.
- 12 J.-H. Park, J. M. Cox-Ganser, K. Kreiss, S. K. White and C. Y. Rao, Hydrophilic Fungi and Ergosterol Associated with Respiratory Illness in a Water-Damaged Building, *Environ. Health Perspect.*, 2008, **116**, 45–50.
- 13 M. J. Ege, M. Mayer, A.-C. Normand, J. Genuneit, W. O. C. M. Cookson, C. Braun-Fahrlander, *et al.*, Exposure to Environmental Microorganisms and Childhood Asthma, *N. Engl. J. Med.*, 2011, **364**(8), 701–709.
- 14 A. Pringle, Asthma and the Diversity of Fungal Spores in Air, *PLoS Pathog.*, 2013, **9**(6), e1003371.
- 15 A. Beigelman, G. M. Weinstock and L. B. Bacharier, The relationships between environmental bacterial exposure, airway bacterial colonization, and asthma, *Curr. Opin. Allergy Clin. Immunol.*, 2014, **14**(2), 137–142.
- 16 R. A. Sharpe, N. Bearman, C. R. Thornton, K. Husk and N. J. Osborne, Indoor fungal diversity and asthma: A meta-analysis and systematic review of risk factors, *J. Allergy Clin. Immunol.*, 2015, **135**(1), 110–122.
- 17 D. W. Denning, B. R. O'Driscoll, C. M. Hogaboam, P. Bowyer and R. M. Niven, The link between fungi and severe asthma: a summary of the evidence, *Eur. Respir. J.*, 2006, **27**, 615–626.
- 18 R. L. Kepner Jr and J. R. Pratt, Use of fluorochromes for direct enumeration of total bacteria in environmental samples: Past and present, *Microbiol. Rev.*, 1994, **58**, 603–615.
- 19 P. H. Kaye, W. R. Stanley, E. Hirst, E. V. Foot, K. L. Baxter and S. J. Barrington, Single particle multichannel bio-aerosol fluorescence sensor, *Opt. Express*, 2005, **13**(10), 3583–3593.
- 20 E. Toprak and M. Schnaiter, Fluorescent biological aerosol particles measured with the Waveband Integrated Bioaerosol Sensor WIBS-4: Laboratory tests combined with a one year field study, *Atmos. Chem. Phys.*, 2013, **13**, 225–243.
- 21 P. H. Kaye, J. E. Barton, E. Hirst and J. M. Clark, Simultaneous light scattering and intrinsic fluorescence measurement for the classification of airborne particles, *Appl. Opt.*, 2000, **39**(21), 3738–3745.
- 22 M. Ila Gosselin, C. M. Rathnayake, I. Crawford, C. Pöhlker, J. Fröhlich-Nowoisky, B. Schmer, *et al.*, Fluorescent bioaerosol particle, molecular tracer, and fungal spore concentrations during dry and rainy periods in a semi-arid forest, *Atmos. Chem. Phys.*, 2016, **16**, 15165–15184.
- 23 C. Pöhlker, J. A. Huffman and U. Pöschl, Autofluorescence of atmospheric bioaerosols – fluorescent biomolecules and potential interferences, *Atmos. Meas. Tech.*, 2012, **5**(1), 37–71.
- 24 J. A. Huffman, A. E. Perring, N. J. Savage, B. Clot, B. Crouzy, F. Tummon, *et al.*, Real-time sensing of bioaerosols: Review and current perspectives, *Aerosol Sci. Technol.*, 2020, **54**, 465–495.
- 25 US EPA Office of Air and Radiation, *Report to Congress on Indoor Air Quality: Volume II -Assessment and control of indoor air pollution*, Washington, DC, 1989.
- 26 P. L. Jenkins, T. J. Phillips, E. J. Mulberg and S. P. Hui, Activity patterns of Californians: Use of and proximity to indoor pollutant sources, *Atmos. Environ., Part A*, 1992, **26**, 2141–2148.
- 27 N. E. Klepeis, W. C. Nelson, W. R. Ott, J. P. Robinson, A. M. Tsang, P. Switzer, *et al.*, The National Human Activity Pattern Survey (NHAPS): a resource for assessing exposure to environmental pollutants, *J. Exposure Anal. Environ. Epidemiol.*, 2001, **11**, 231–252.
- 28 D. Hospodsky, J. Qian, W. W. Nazaroff, N. Yamamoto, K. Bibby, H. Rismani-Yazdi, *et al.*, Human occupancy as a source of indoor airborne bacteria, *PLoS One*, 2012, **7**, e34867.
- 29 J. F. Meadow, A. E. Altrichter, S. W. Kembel, J. Kline, G. Mhuireach, M. Moriyama, *et al.*, Indoor airborne bacterial communities are influenced by ventilation, occupancy, and outdoor air source, *Indoor Air*, 2014, **24**, 41–48.
- 30 R. I. Adams, Y. Tian, J. W. Taylor, T. D. Bruns, A. Hyvärinen and M. Täubel, Passive dust collectors for assessing airborne microbial material, *Microbiome*, 2015, **3**(1), 46.
- 31 Y. Tian, Y. Liu, P. K. Misztal, J. Xiong, C. M. Arata, A. H. Goldstein, *et al.*, Fluorescent biological aerosol particles: Concentrations, emissions, and exposures in a northern California residence, *Indoor Air*, 2018, **28**, 559–571.
- 32 J. D. Berman and K. Ebisu, Changes in U.S. air pollution during the COVID-19 pandemic, *Sci. Total Environ.*, 2020, **739**, 139864.
- 33 M. A. Cole, R. J. R. Elliott and B. Liu, The Impact of the Wuhan Covid-19 Lockdown on Air Pollution and Health: A Machine Learning and Augmented Synthetic Control Approach, *Environmental Resource Economics*, 2020, **76**, 553–580.
- 34 R. H. Rana, S. A. Keramat and J. Gow, A Systematic Literature Review of the Impact of COVID-19 Lockdowns on Air Quality in China, *Aerosol Air Qual. Res.*, 2021, **21**, 3283–3292.
- 35 J. Li, M. P. Wan, S. Schiavon, K. W. Tham, S. Zuraimi, J. Xiong, *et al.*, Size-resolved dynamics of indoor and outdoor fluorescent biological aerosol particles in a bedroom: A one-month case study in Singapore, *Indoor Air*, 2020, **30**, 942–954.
- 36 V. D. Nathu, J. Virkutyte, M. B. Rao, M. Nieto-caballero, M. Hernandez and T. Re, Direct-read fluorescence-based measurements of bioaerosol exposure in home healthcare, *Int. J. Environ. Res. Public Health*, 2022, **1**–16.
- 37 M. Nieto-Caballero, O. M. Gomez, R. Shaughnessy and M. Hernandez, Aerosol fluorescence, airborne hexosaminidase, and quantitative genomics distinguish

- reductions in airborne fungal loads following major school renovations, *Indoor Air*, 2022, **32**(1), e12975.
- 38 A. M. Gabey, M. W. Gallagher, J. Whitehead, J. R. Dorsey, P. H. Kaye and W. R. Stanley, Measurements and comparison of primary biological aerosol above and below a tropical forest canopy using a dual channel fluorescence spectrometer, *Atmos. Chem. Phys.*, 2010, **10**(10), 4453–4466.
 - 39 N. J. Savage, C. E. Krentz, T. Könemann, T. T. Han, G. Mainelis, C. Pöhlker, *et al.*, Systematic characterization and fluorescence threshold strategies for the wideband integrated bioaerosol sensor (WIBS) using size-resolved biological and interfering particles, *Atmos. Meas. Tech.*, 2017, **10**(11), 4279–4302.
 - 40 A. E. Perring, J. P. Schwarz, D. Baumgardner, M. T. Hernandez, D. V. Spracklen, C. L. Heald, *et al.*, Airborne observations of regional variation in fluorescent aerosol across the United States, *J. Geophys. Res.: Atmos.*, 2015, **120**, 1153–1170.
 - 41 J. Qian, D. Hospodsky, N. Yamamoto, W. W. Nazaroff and J. Peccia, Indoor Air, *Size-resolved emission rates of airborne bacteria and fungi in an occupied classroom*, 2012, **22**, 339–351.
 - 42 S. S. Patra, T. Wu, D. N. Wagner, J. Jiang and B. E. Boor, Real-time measurements of fluorescent aerosol particles in a living laboratory office under variable human occupancy and ventilation conditions, *Building Environment*, 2021, **205**, 108249.
 - 43 S. Faridi, M. S. Hassanvand, K. Naddafi, M. Yunesian, R. Nabizadeh and M. H. Sowlat, *et al.*, Indoor/outdoor relationships of bioaerosol concentrations in a retirement home and a school dormitory, *Environ. Sci. Pollut. Res. Int.*, ed. J.-F. Cholle, M. Treilhou, M. Couderchet, M. Treilhou, J.-F. Cholle and M. Couderchet, Springer Berlin Heidelberg, Berlin/Heidelberg, 2015, vol. 22, pp. 8190–8200.
 - 44 J. Qian and A. R. Ferro, Resuspension of Dust Particles in a Chamber and Associated Environmental Factors, *Aerosol Sci. Technol.*, 2008, **vol. 42**, 566–578.
 - 45 T. Lee, S. A. Grinshpun, D. Martuzevicius, A. Adhikari, C. M. Crawford, J. Luo, *et al.*, Relationship between indoor and outdoor bioaerosols collected with a button inhalable aerosol sampler in urban homes, *Indoor Air*, 2006, **16**(1), 37–47.
 - 46 Department of Statistics Singapore, *SingStat Table Builder*, 2022, cited 2022 May 4, pp. 1–5, available from: <http://www.tablebuilder.singstat.gov.sg/publicfacing/mainMenu.action>.
 - 47 M. S. Zuraïmi and K. W. Tham, Indoor air quality and its determinants in tropical child care centers, *Atmos. Environ.*, 2008, **42**, 2225–2239.
 - 48 A. R. Ferro, R. J. Kopperud and L. M. Hildemann, Source Strengths for Indoor Human Activities that Resuspend Particulate Matter, *Environ. Sci. Technol.*, 2004, **38**, 1759–1764.
 - 49 J. F. Meadow, A. E. Altrichter, S. W. Kembel, J. Kline, G. Mhuireach, M. Moriyama, *et al.*, Indoor airborne bacterial communities are influenced by ventilation, occupancy, and outdoor air source, *Indoor Air*, 2014, **24**, 41–48.
 - 50 R. I. Adams, S. Bhangar, W. Pasut, E. A. Arens, J. W. Taylor, S. E. Lindow, *et al.*, Chamber Bioaerosol Study: Outdoor Air and Human Occupants as Sources of Indoor Airborne Microbes, *PLoS One*, 2015, **10**, e0128022.
 - 51 S. Bhangar, R. I. Adams, W. Pasut, J. A. Huffman, E. A. Arens, J. W. Taylor, *et al.*, Chamber bioaerosol study: human emissions of size-resolved fluorescent biological aerosol particles, *Indoor Air*, 2016, **26**, 193–206.
 - 52 H. Priyamvada, C. Priyanka, R. K. Singh, M. Akila, R. Ravikrishna and S. S. Gunthe, Assessment of PM and bioaerosols at diverse indoor environments in a southern tropical Indian region, *Build Environ.*, 2018, **137**, 215–225.
 - 53 R. Becher, J. Øvrevik, P. E. Schwarze, S. Nilsen, J. K. Hongslo and J. V. Bakke, Do Carpets Impair Indoor Air Quality and Cause Adverse Health Outcomes: A Review, *Int. J. Environ. Res. Public Health*, 2018, **15**, 184.
 - 54 S. Yang, G. Bekö, P. Wargocki, J. Williams and D. Licina, Human Emissions of Size-Resolved Fluorescent Aerosol Particles: Influence of Personal and Environmental Factors, *Environ. Sci. Technol.*, 2021, **55**, 509–518.
 - 55 C. M. O'Gorman and H. T. Fuller, Prevalence of culturable airborne spores of selected allergenic and pathogenic fungi in outdoor air, *Atmos. Environ.*, 2008, **42**(18), 4355–4368.
 - 56 I. Crawford, N. H. Robinson, M. J. Flynn, V. E. Foot, M. W. Gallagher, J. A. Huffman, *et al.*, Characterisation of bioaerosol emissions from a Colorado pine forest: Results from the beachon-rombas experiment, *Atmos. Chem. Phys.*, 2014, **14**(16), 8559–8578.
 - 57 B. G. Shelton, K. H. Kirkland, W. D. Flanders and G. K. Morris, Profiles of airborne fungi in buildings and outdoor environments in the United States, *Appl. Environ. Microbiol.*, 2002, **68**(4), 1743–1753.
 - 58 B. Graham, P. Guyon, W. Maenhaut, P. E. Taylor, M. Ebert, S. Matthias-Maser, *et al.*, Composition and diurnal variability of the natural Amazonian aerosol, *J. Geophys. Res.: Atmos.*, 2003, **108**, 4765.
 - 59 R. M. Garland, O. Schmid, A. Nowak, P. Achtert, A. Wiedensohler, S. S. Gunthe, *et al.*, Aerosol optical properties observed during Campaign of Air Quality Research in Beijing 2006 (CAREBeijing-2006): Characteristic differences between the inflow and outflow of Beijing city air, *J. Geophys. Res.: Atmos.*, 2009, **114**, D00G04.
 - 60 A. I. Calvo, D. Baumgardner, A. Castro, R. M. Valencia-barrera, F. Oduber, C. Blanco-alegre, *et al.*, Daily behavior of urban Fluorescing Aerosol Particles in northwest Spain, *Atmos. Environ.*, 2018, **184**, 262–277.
 - 61 R. Jaenicke, S. Matthias-Maser and S. Gruber, Omnipresence of biological material in the atmosphere, *Environ. Chem.*, 2007, **4**, 217–220.
 - 62 J. A. Huffman, B. Sinha, R. M. Garland, A. Snee-Pollmann, S. S. Gunthe, P. Artaxo, *et al.*, Size distributions and temporal variations of biological aerosol particles in the Amazon rainforest characterized by microscopy and real-time UV-APS fluorescence techniques during AMAZE-08, *Atmos. Chem. Phys.*, 2012, **12**, 11997–12019.

- 63 M. Hernandez, A. E. Perring, K. McCabe, G. Kok, G. Granger and D. Baumgardner, Chamber catalogues of optical and fluorescent signatures distinguish bioaerosol classes, *Atmos. Meas. Tech.*, 2016, **9**, 3283–3292.
- 64 S. Bhangar, J. A. Huffman and W. W. Nazaroff, Size-resolved fluorescent biological aerosol particle concentrations and occupant emissions in a university classroom, *Indoor Air*, 2014, **24**, 604–617.
- 65 A. Handorean, C. E. Robertson, J. K. Harris, D. Frank, N. Hull, C. Kotter, *et al.*, Microbial aerosol liberation from soiled textiles isolated during routine residuals handling in a modern health care setting, *Microbiome*, 2015, **3**, 72.
- 66 A. Handorean, C. E. Robertson, J. K. Harris, D. Frank, N. Hull, C. Kotter, *et al.*, Microbial aerosol liberation from soiled textiles isolated during routine residuals handling in a modern health care setting, *Microbiome*, 2015, **3**, 72.
- 67 J. Zhou, W. Fang, Q. Cao, L. Yang, V. W. C. Chang and W. W. Nazaroff, Influence of moisturizer and relative humidity on human emissions of fluorescent biological aerosol particles, *Indoor Air*, 2017, **27**(3), 587–598.
- 68 J. Douwes, P. Thorne, N. Pearce and D. Heederick, Bioaerosol Health Effects and Exposure Assessment: Progress and Prospects, *Ann. Work Exposures Health*, 2003, **47**(3), 187–200.
- 69 J. Li and F. Tartarini, Changes in Air Quality during the COVID-19 Lockdown in Singapore and Associations with Human Mobility Trends, *Aerosol Air Qual. Res.*, 2020, **20**(8), 1748–1758.
- 70 A. Goel, P. Saxena, S. Sonwani, S. Rathi, A. Srivastava, A. K. Bharti, *et al.*, Health Benefits Due to Reduction in Respirable Particulates during COVID-19 Lockdown in India, *Aerosol Air Qual. Res.*, 2021, **21**, 200460.
- 71 M. Soni, S. Verma, H. Jethava, S. Payra, L. Lamsal, P. Gupta, *et al.*, Impact of COVID-19 on the Air Quality over China and India Using Long-term (2009–2020) Multi-satellite Data, *Aerosol Air Qual. Res.*, 2021, **21**(3), 200295.
- 72 M. Filonchyk, V. Hurynovich and H. Yan, Impact of COVID-19 Pandemic on Air Pollution in Poland Based on Surface Measurements and Satellite Data, *Aerosol Air Qual. Res.*, 2021, **21**, 200472.
- 73 E. Ezani, P. Brimblecombe, Z. Hanan Asha'ari, A. A. Fazil, S. N. Syed Ismail, Z. T. Ahmad Ramly, *et al.*, Indoor and Outdoor Exposure to PM_{2.5} during COVID-19 Lockdown in Suburban Malaysia, *Aerosol Air Qual. Res.*, 2021, **21**(3), 200476.
- 74 R. Zalakeviciute, R. Vasquez, D. Bayas, A. Buenano, D. Mejia, R. Zegarra, *et al.*, Drastic Improvements in Air Quality in Ecuador during the COVID-19 Outbreak, *Aerosol Air Qual. Res.*, 2020, **20**(8), 1783–1792.
- 75 A. R. Naeger and K. Murphy, Impact of COVID-19 Containment Measures on Air Pollution in California, *Aerosol Air Qual. Res.*, 2020, **20**(10), 2025–2034.
- 76 S. Faridi, F. Yousefian, S. Niazi, M. R. Ghalhari, M. S. Hassanvand and K. Naddafi, Impact of SARS-CoV-2 on Ambient Air Particulate Matter in Tehran, *Aerosol Air Qual. Res.*, 2020, **20**(8), 1805–1811.
- 77 Z. Li, J. Meng, L. Zhou, R. Zhou, M. Fu, Y. Wang, *et al.*, Impact of the COVID-19 Event on the Characteristics of Atmospheric Single Particle in the Northern China, *Aerosol Air Qual. Res.*, 2020, **20**(8), 1716–1726.
- 78 W. Du and G. Wang, Indoor Air Pollution was Nonnegligible during COVID-19 Lockdown, *Aerosol Air Qual. Res.*, 2020, **20**(9), 1851–1855.
- 79 N. S. Represa, L. S. Della Ceca, G. Abril, M. F. García Ferreyra and C. M. Scavuzzo, Atmospheric Pollutants Assessment during the COVID-19 Lockdown Using Remote Sensing and Ground-based Measurements in Buenos Aires, Argentina, *Aerosol Air Qual. Res.*, 2021, **21**(3), 200486.
- 80 J. Kaewrat and R. Janta, Effect of COVID-19 Prevention Measures on Air Quality in Thailand, *Aerosol Air Qual. Res.*, 2021, **21**(3), 200344.
- 81 J. Li, H. Yang, S. Zha, N. Yu, X. Liu and R. Sun, Effects of COVID-19 Emergency Response Levels on Air Quality in the Guangdong-Hong Kong-Macao Greater Bay Area, China, *Aerosol Air Qual. Res.*, 2021, **21**(2), 200416.